Catalytic activity of ZSM-11 zeolites modified with metal cations for the ethane conversion

Oscar A. Anunziata *, Griselda A. Eimer and Liliana B. Pierella

CITeQ (Centro de Investigación y Tecnología Química), Facultad Córdoba, Universidad Tecnológica Nacional, CC36 Suc16(5016), Córdoba, Argentina
E-mail: oanunziata@scdt.frc.utn.edu.ar

ZSM-11 zeolite samples differing by their active sites (H^+ and different metal cations) have been studied in the transformation of ethane into aromatic hydrocarbons. A relationship between Lewis sites increasing–aromatization capacity and possible reaction steps have been suggested.

KEY WORDS: ethane conversion; aromatic hydrocarbons; active sites; modified zeolites

1. Introduction

Ethane (C_2) is a component of a variety of refinery gases. Natural gas (NG) may contain C_2 from traces up to more than 10%. According to thermodynamic data, transformation of C_2 requires higher temperatures whereas aromatization of propane (C_3) and higher alkanes can be carried out at lower temperatures than 500 °C. Thus, the activation of ethane results in an intriguing subject. Pentasil zeolites loaded with metal cations, such as gallium and zinc have been successfully used for activation and conversion of light alkanes into aromatic hydrocarbons (AH). Ono et al. [1] studied the C_2 transformation indicating that incorporating gallium or zinc into ZSM-5 greatly enhances the activation of ethane and is essential for the formation of aromatics from C_2. Solymosi et al. [2] reported excellent C_2 conversion levels, about 75%, on MoO_3/ZSM-5 catalyst into benzene, at the high reaction temperature of 700 °C. Choudhary et al. [3] studied direct aromatization of NG over gallium-zeolites, reporting conversion of C_{2+} hydrocarbons in 70% at 600 °C. In our previous papers, we have reported that Zn-ZSM-11 and Mo-ZSM-11 show an excellent catalytic behavior for aromatization of NG and light paraffins [4–8]. Here, we describe C_2 transformation over ZSM-11 zeolites modified with different metal cations and suggest possible reaction steps with special emphasis on the relationship between the nature of the active site and the mode of C_2 activation.

2. Experimental

ZSM-11 zeolites (Si/Al = 17) were synthesized by hydrothermal crystallization in Na_2O–Al_2O_3–SiO_2 systems, in the presence of tetrabutylammonium hydroxide as template [7]. Zn-ZSM-11(20), Zn-ZSM-11(50) and Zn-ZSM-11(80), that presented 20, 50 and 80% ionic exchange percentages, respectively, were prepared by ion exchange of NH_4-zeolite with 0.05 M zinc nitrate solution by refluxing. The cations Pb^{2+}, Fe^{3+} and Cu^{2+} were incorporated to Zn-ZSM-11(50) by ion exchange, reaching a total ionic exchange percentage of 80%. Mo-ZSM-11 was prepared by impregnating NH_4-zeolite with aqueous ammonium heptamolybdate solutions to yield a 2 wt% of Mo, whereas Mo–Zn-ZSM-11 was prepared by impregnating Zn-ZSM-11(50) with aqueous ammonium heptamolybdate solutions to yield a 1 wt% of Mo. Finally, the samples were dried at 110 °C and calcined at 500 °C overnight. Table 1 lists the chemical composition and total surface area obtained by BET of the catalytic materials used in this work. All the catalysts showed high levels of purity and crystallinity obtained by XRD. Infrared measurements were performed on a Jasco 5300 FT-IR spectrometer. The samples were pressed into self-supporting wafers (8–10 mg/cm^2) and pyridine (3 Torr) was adsorbed at room temperature and desorbed at 400 °C and 10^{-4} Torr. IR data for chemisorbed pyridine interacting with Brønsted acid sites and Lewis sites in zeolite allowed us to determine the concentration of Brønsted and Lewis

Table 1
Chemical composition and total surface area of the catalytic materials used in this work.

Catalyst	Cation (mol/cell unit)	Cation (wt%)	Surface area (m^2/g)
H-ZSM-11	–	–	379
Zn-ZSM-11(20)	Zn 0.54	0.6	356
Zn-ZSM-11(50)	Zn 1.33	1.5	348
Zn–Pb-ZSM-11	Zn 1.33, Pb 0.8	Zn 1.5, Pb 2.8	350
Zn–Mo-ZSM-11	Zn 1.33, Mo 0.61	Zn 1.5, Mo 1	331
Zn–Cu-ZSM-11	Zn 1.33, Cu 0.8	Zn 1.5, Cu 0.87	312
Zn–Fe-ZSM-11	Zn 1.33, Fe 0.53	Zn 1.5, Fe 0.5	319
Zn-ZSM-11(80)	Zn 2.13	Zn 2.4	347
Mo-ZSM-11	Mo 1.22	Mo 2	335

* To whom correspondence should be addressed.

Table 2
FTIR results of pyridine retained after desorption at 400 °C and 10^{-4} Torr by 4 h.

	Catalyst[a]								
	(1)	(2)	(3)	(4)	(5)	(6)	(7)	(8)	(9)
BS[b]	0.0260	0.0210	0.0090	0.0040	0.0090	0.0071	0.0200	0.0072	0.0220
LS[c]	0.0025	0.0127	0.0300	0.0333	0.0439	0.0351	0.029	0.0440	0.0480

[a] (1) H-ZSM-11, (2) Zn-ZSM-11(20), (3) Zn-ZSM-11(50), (4) Zn–Pb-ZSM-11, (5) Zn–Mo-ZSM-11, (6) Zn–Cu-ZSM-11, (7) Zn–Fe-ZSM-11, (8) Zn-ZSM-11(80), (9) Mo-ZSM-11.
[b] BS = Brønsted sites in absorbance units.
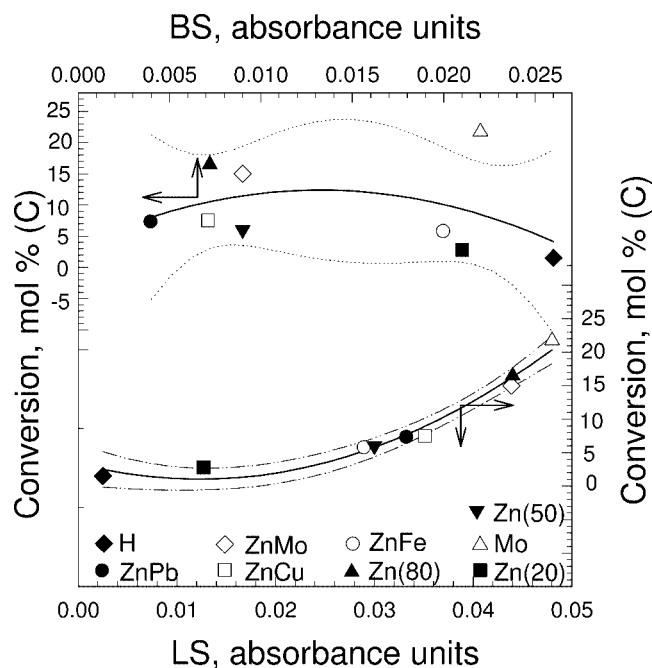[c] LS = Lewis sites in absorbance units.

Figure 1. Ethane conversion *vs.* Brønsted–Lewis sites at 30 g h/mol and 550 °C.

Figure 2. AH selectivity *vs.* Brønsted–Lewis sites at 30 g h/mol and 550 °C.

strong acid sites of zeolites modified with different metal cations. Catalytic reactions were carried out in a continuous-flow fixed-bed reactor which was on line with a gas chromatograph equipped with FID detector and operated at atmospheric pressure. All the products were withdrawn periodically from the outlet of the reactor and analyzed by using a 2.2 m Porapak Q column. Ethane was supplied by AGA (USA) with more than 99.97% purity. The operating conditions were: temperature $T = 550$–650 °C, contact time $W/F = 2$–60 g h/mol and time-on-stream TOS $= 20$–300 min. Conversion and selectivity to reaction products were expressed on a carbon-atom basis.

3. Results and discussion

Table 2 shows the FTIR results of pyridine retained for the catalysts after its desorption at 400 °C and 10^{-4} Torr by 4 h. The data listed are called by us as "strong Brønsted and Lewis sites", in absorbance units normalized for zeolite wafers of 10 mg.

In figures 1, 2, 3 and 4 conversion and selectivity to aromatic hydrocarbons (AH), ethylene ($C_2^=$) and methane (C_1)
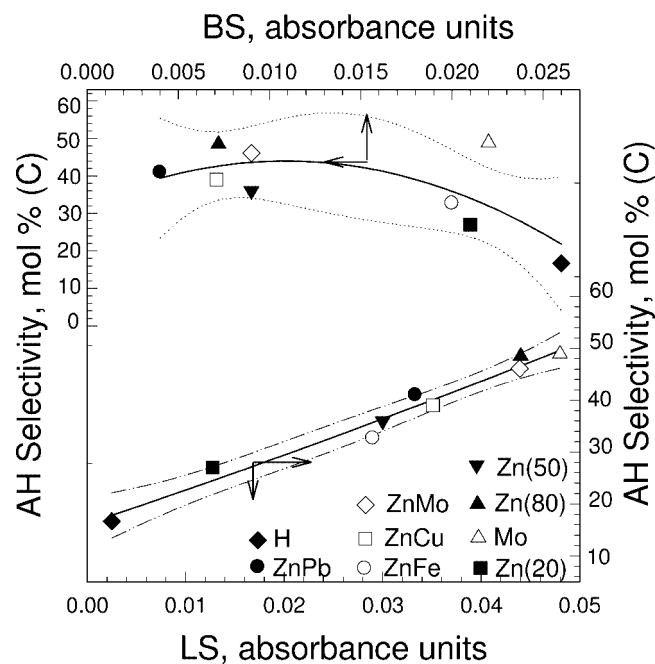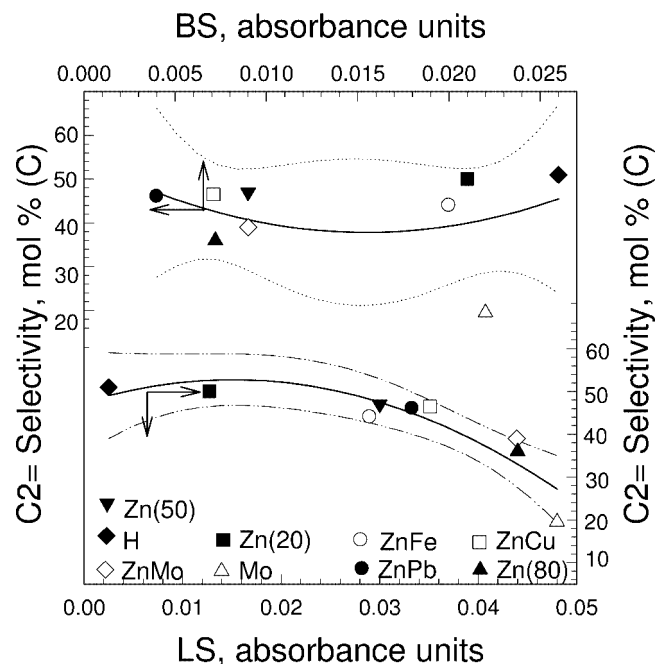

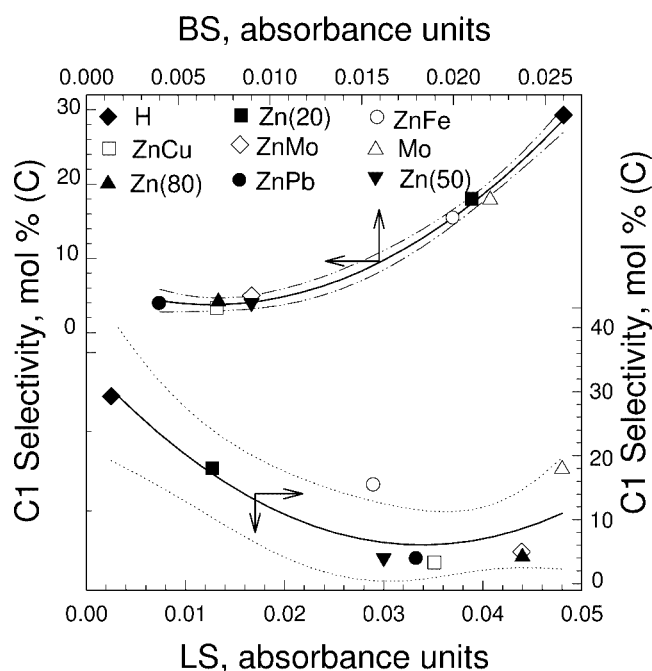Figure 3. $C_2^=$ selectivity *vs.* Brønsted–Lewis sites at 30 g h/mol and 550 °C.

Figure 4. C_1 selectivity *vs.* Brønsted–Lewis sites at 30 g h/mol and 550 °C.

respectively are plotted against Lewis and Brønsted sites for the zeolites evaluated at 550 °C, $W/F = 30$ g h/mol, and TOS = 20 min. The metal cations responsible for the different nature of the active sites and fitted curves confidence intervals within 95% also are indicated in these figures. It can be seen in figures 1 and 2 that over the proton form of ZSM-11, conversion and selectivity to aromatics are very low and there is a direct relationship between increasing Lewis sites of different metal-promoted catalysts and increase of ZSM-11 conversion and AH selectivity. Moreover, the additional metal loading on the Zn-ZSM-11(50), except for Zn–Fe-ZSM-11, generate new Lewis sites showing consequently, positive effect on ethane conversion and aromatics selectivity. Meanwhile, the tendency to decreasing of $C_2^=$ and C_1 selectivity when Lewis sites increase can be observed in figures 3 and 4. The confidence intervals for these curves are not optimal (mainly for figure 4) due to two points corresponding to Mo-ZSM-11 and Zn-Fe-ZSM-11 catalysts. Such catalysts show an anomalous high selectivity to C_1 if we take account of their Lewis sites concentration but a good relation with their Brønsted sites concentration. This fact could be attributed to the presence of a high number of Brønsted sites on these catalysts given the particular mode of introduction of metal cation. The incorporation of Fe^{3+} cation on Zn-ZSM-11 could generate Brønsted sites without increasing of Lewis sites. Recently we studied the synthesis, characterization and catalytic activity of $Fe^{(2+,3+)}$-BEA and $Fe^{(2+,3+)}$-MFI zeolites. The FTIR analysis of the amount of Brønsted and Lewis acid sites, indicated that zeolites with Fe^{2+} as counter ion show greater proportion of Lewis sites than the zeolite with Fe^{3+} [9]. The nature of Mo active sites of Mo-zeolites (high concentration of both Brønsted and Lewis sites) has been reported by us elsewhere [8,10,11]. FTIR spectra of pyridine-Lewis sites from H-ZSM and Mo-

ZSM desorbed at 400 °C and 10^{-4} Torr showed that the new Lewis band at 1446 cm^{-1} appears in Mo-ZSM samples well differentiated from Lewis sites (1454 cm^{-1}) due to Al in the framework [11]. Furthermore, as it can be seen in figure 4, a direct relationship between increase of C_1 selectivity and enhancing Brønsted sites could be confirmed. Then, we suggest that the nature of the active sites (Brønsted or Lewis) is responsible for a change in interaction between C_2 and catalyst. High Lewis sites would produce high concentrations of hydrogen acceptor species and dehydrogenation would be favorable leading to high levels of conversion and AH. On the other hand, Brønsted sites would promote the cracking activity and production of C_1 through protonation of reactive and formation of carbonium cation species.

The Zn-ZSM-11(80), Mo-ZSM-11 and Zn-Mo-ZSM-11 catalysts reached the largest concentration of Lewis sites and consequently the highest levels of conversion and aromatics production. Figures 5, 6 and 7 show the selectivity behavior of the reaction products for C_2 transformation as TOS approaches zero at 550 °C on Zn-ZSM-11(80), Mo-ZSM-11 and Zn–Mo-ZSM-11, respectively, according to the results obtained by using the standard optimum performance envelope technique [7,8]. In these figures, product formation rates are plotted against turnover number (TON) and ethane conversion is also indicated in an auxiliary axis "*x*". Ethylene appears as an unstable primary product and aromatics are found as stable secondary products. C_1 appears as secondary stable product, which shows it is not produced by cracking of ethane and does not undergo secondary transformation. In contrast, Solymosi and Szöke [2] reported that the formation of C_1 proceeds from C_2 over MoO_3-ZSM-5 and Choudhary et al. [3] indicated that C_1 can be produced by cracking of propane or butane, by hydrocracking or hydrogenolysis of C_2, C_3 or C_4 and by dealkylation of aromatics. In addition, propane would be a stable secondary product resulting from butane cracking. Butane, butene and propene are unstable secondary products, which arise from propene polymerization. Mo or Zn cations loaded over ZSM-11 zeolite could act as hydride abstractors in the ethane activation since they leave a high number of Lewis sites (table 1). The function of metal species would be the dehydrogenation of ethane into ethylene and of naphthenic intermediates into aromatics. The first step would be the direct abstraction of a hydride from ethane, producing a carbenium-like surface species (ethyl-carbenium ion) through electron-donor–acceptor adduct (EDA) formation, and then by deprotonation ethylene [7,8]. Then, ethylene could react with other carbenium C_2 species, undergoing numerous secondary transformations. On the other hand, the presence of strong Lewis sites in the catalyst prevents hydrogenation of intermediate alkenes, which would be efficiently introduced into the polymerization, cyclization, dehydrogenation and aromatization complex mechanism. If we compare figures 5, 6 and 7, it can be seen that the turnover number and products formation rate is influenced by the nature of metal species loaded over the catalyst. At the same levels of conversion, Mo cation leaves
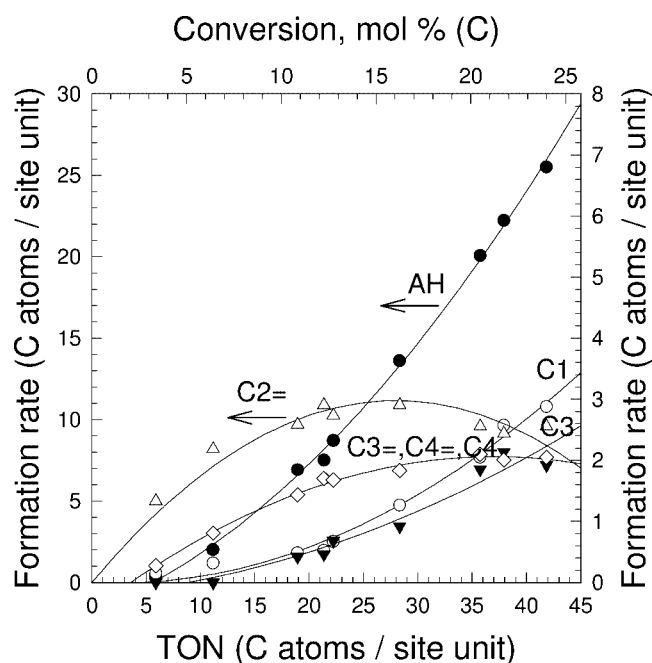
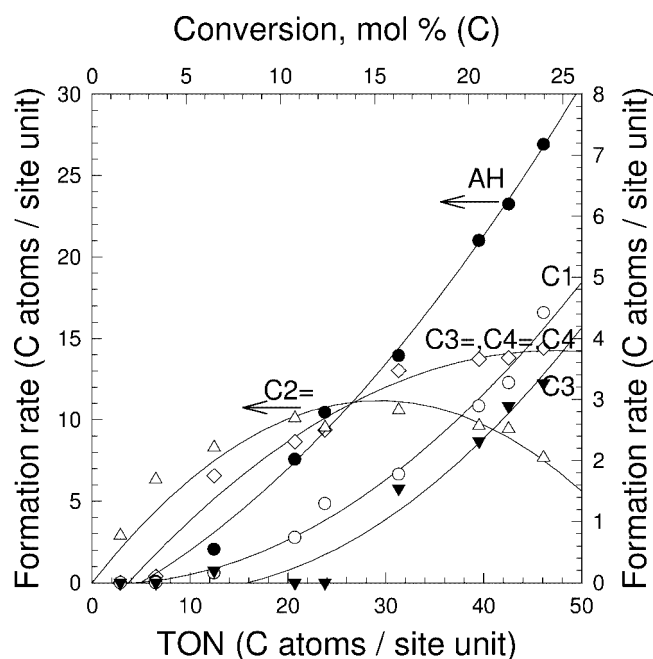Figure 5. Products formation rate *vs.* TON over Zn-ZSM-11, at 550 °C.

Figure 7. Products formation rate *vs.* TON over Zn–Mo-ZSM-11, at 550 °C.
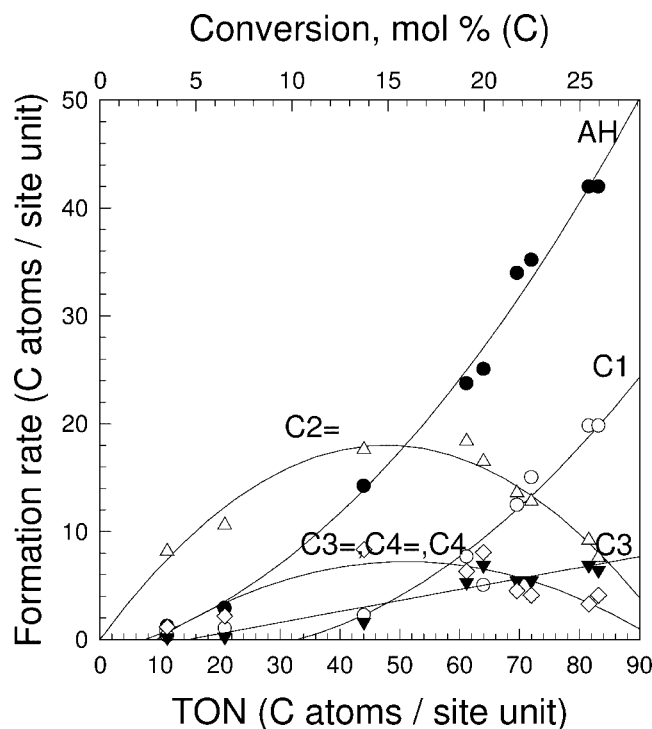

Figure 6. Products formation rate *vs.* TON over Mo-ZSM-11, at 550 °C.

a higher TON and products formation rate than Zn cation. In this way, Mo appears as the metal species more effective for the ethane activation and aromatization. *In situ* and *ex situ* XANES study of nanodispersed Mo species in zeolites synthesized through the method described in this work, has been reported by us elsewhere [10,11]. Mo K-edge XANES experiments on Mo-containing zeolites at low Mo loading (1 and 2 wt% of Mo on H-ZSM-11, H-BETA and H-ZSM-5

catalysts) were performed *ex situ* as function of sample calcination temperature in air (in the range 500–700 °C) or *in situ* at 600 and 700 °C under N_2 flow. At 700 °C in N_2, the samples almost reached 100% of NN-4 fraction, provided they stay long enough in this state. This fraction cannot be extra-framework $Al_2(MoO_4)_3$ since, in such a case, the reversibility should imply that this compound decompose with decreasing temperature in air. Moreover, a MoO_3-like species, which is not present, does not develop in air at higher calcination temperatures as could have been expected [11]. Then, these results show a four-fold oxygen coordination for the incorporated Mo species in the activated state and a high efficiency of the preparation method for Mo incorporation as counter-ion. The combination of these results with EXAFS and EDX/XPS measurements are in agreement with a total Mo exchange inside the channels of the zeolites [10].

In addition, the influence of time-on-stream on the C_2 transformation was examined over Mo, Zn and Zn–Mo loaded ZSM-11 zeolites in the range 20 to 300 min at $W/F = 30$ g h/mol and 550 °C. The C_2 conversion remained almost constant on the whole range of times on stream studied. Selectivity to aromatics and C_1 decreased very lightly with reaction time whereas $C_2^=$ selectivity increased also lightly. It can be suggested that ZSM-11 zeolite loaded with Mo and Zn cations would be deactivated very slowly by coke deposition on active sites. At the beginning, the deactivation would occur over active sites for intermediate oligomerization.

Moreover, the effect of temperature on the C_2 conversion and selectivity to reaction products over Mo-ZSM-11, Zn-ZSM-11(80) and Zn–Mo-ZSM-11 at $W/F = 30$ g h/mol, TOS = 20 min and temperatures between 550 and 700 °C has been studied. As the temperature increased, conversion, aromatic hydrocarbons and C_1 selectivity increased

whereas $C_2^=$ decreased being introduced into the polymerization, cyclization, dehydrogenation and aromatization complex mechanism. C_1 increased with temperature to balance the hydrogen content in the feed and would be formed *via* cracking of higher aliphatic intermediates and demethylation of aromatics in the process. The high selectivity to aromatic hydrocarbons even at low ethane conversion indicated that the precursor species are easily aromatized. The conversion and aromatics selectivity reached levels of 85 and 62%, respectively, over Mo-ZSM-11 and levels of 60 and 68%, respectively, over Zn-ZSM-11 at 650 °C and $W/F = 30$ g h/mol. These results are consistent with those reported by Ono *et al.* [2] for ethane conversion over Zn-ZSM-5.

4. Conclusions

Ethane aromatization is strongly influenced by the nature and concentration of the active sites on the catalyst. So, the Lewis sites increasing generated by the introduction of different metal species over zeolites favors such transformation. The introduction of additional metal such as Fe, Cu and Pb into Zn-ZSM-11(50) (50% total ionic exchange) to reach 80% total ionic exchange, allowed increasing slightly the conversion of C_2. The incorporation of such cations would be less effective for activation and aromatization of C_2 since they would fail to reach a high concentration of Lewis sites in the catalyst. ZSM-11 zeolites loaded with metal cations such as molybdenum or zinc, Mo-ZSM-11, Zn-ZSM-11(80) and Zn–Mo-ZSM-11, which present the highest concentration of Lewis sites enhanced to a large extent the C_2 activation and production of aromatics, improving the effective aromatization of intermediates. Therefore, it can be confirmed that Lewis sites are responsible for the creation of dehydrogenation and aromatization centers owing to its capacity for the abstraction of hydrides and formation of carbenium surface ion intermediates. On the other hand, the catalyst with high concentration of Brønsted sites present high C_1 selectivity verifying that such sites would promote centers of protonation and cracking of the reactant molecules.

Acknowledgement

References

[1] Y. Ono, Catal. Rev. Sci. Eng. 34 (3) (1992) 179.

[2] F. Solymosi and A. Szöke, Appl. Catal. A 166 (1) (1998) 225.

[3] V. Choudhary, A. Kinage and T. Choudhary, Appl. Catal. A 162 (1997) 239.

[4] O. Anunziata, G. Eimer and L. Pierella, Appl. Catal. A 190 (2000) 169.

[5] L. Pierella, G. Eimer and O. Anunziata, *NGCV*, Stud. Surf. Sci. Catal., Vol. 119 (1998) p. 235.

[6] O. Anunziata, G. Eimer and L. Pierella, Catal. Lett. 58 (1999) 235.

[7] L. Pierella, G. Eimer and O. Anunziata, React. Kinet. Catal. Lett. 63 (1998) 271.

[8] O. Anunziata, G. Eimer and L. Pierella, Appl. Catal. A 182 (1999) 267.

[9] O. Anunziata, L. Pierella, E. Lede and F. Requejo, Stud. Surf. Sci. Catal. (2001), in press.

[10] M. Renteria, A. Traverse, O. Anunziata, E. Lede, L. Pierella and F. Requejo, J. Synch. Rad. 8 (2001) 631.

[11] F. Requejo, E. Lede, L. Pierella and O. Anunziata, Stud. Surf. Sci. Catal. (2001), in press.